

Probing the dark side: Constraints on the dark energy equation of state from CMB, large scale structure and Type Ia supernovae

Steen Hannestad*

NORDITA, Blegdamsvej 17, DK-2100 Copenhagen, Denmark

Edvard Mörtsell†

Department of Physics, Stockholm University, S - 106 91 Stockholm, Sweden

(Dated: May 6, 2019)

We have reanalysed constraints on the equation of state parameter, $w_Q \equiv P/\rho$, of the dark energy, using several cosmological data sets and relaxing the usual constraint $w_Q \geq -1$. We find that combining Cosmic Microwave Background, large scale structure and Type Ia supernova data yields a non-trivial lower bound on w_Q . At 95.4% confidence we find, assuming a flat geometry of the universe, a bound of $-2.68 < w_Q < -0.78$ if w_Q is taken to be a completely free parameter. Reassuringly we also find that the constraint $w_Q \geq -1$ does not significantly bias the overall allowed region for w_Q . When this constraint is imposed the 95.4% confidence bound is $-1 \leq w_Q < -0.71$. Also, a pure cosmological constant ($w = -1$) is an excellent fit to all available data. Based on simulations of future data from the Planck CMB experiment and the SNAP and SNfactory supernova experiments we estimate that it will be possible to constrain w_Q at the 5% level in the future.

PACS numbers: 98.80.-k, 12.60.-i, 14.80.-j

I. INTRODUCTION

Several independent methods of observation all suggest that most of the energy density in the universe is in the form of a component with negative pressure – dark energy. The simplest possibility for such a component is a cosmological constant which has a constant equation of state $P_Q = -\rho_Q$. However, in the general case the dark energy can have an equation of state which is time-dependent, $P_Q = w_Q(t)\rho_Q$ [1, 2, 3, 4, 5, 6, 7, 8, 9]. Dark energy with a time-dependent equation of state has been invoked to explain the coincidence problem, the fact that the energy density in dark energy is roughly equal to that in dark matter exactly at the present epoch. By coupling a scalar field to matter one can obtain tracking solutions for the time dependence of the dark energy density so that it always follows the dominant energy density component.

Generic to most of these proposed candidates for dark energy is the fact that $w_Q \geq -1$ at all times. This is, e.g., the case for most quintessence models where a scalar field is rolling in a potential (potential driven quintessence). Since most of the plausible models lie in this category, the likelihood analyses which have been used to find w_Q have cut away the region with $w_Q < -1$. From a purely phenomenological point of view this is not justified and can lead to severe bias in parameter determination. This is particularly worrisome because the most recent data set an upper limit on $w_Q < -0.85$ (68% confidence) [10] (see also [11]), but *not* a lower limit. Therefore, if the true model has $w_Q < -1$, the upper bound could be

wrong (and in principle a full analysis could even rule out a cosmological constant as being the dark energy). In fact there are several models which predict a dark energy component with $w_Q < -1$ [12, 13, 14, 15, 16, 17]. This possible bias problem was also discussed in Ref. [18].

In the present paper we reanalyse cosmological data from the Cosmic Microwave Background (CMB), large scale structure (LSS) and Type Ia supernovae (SNe) without the constraint $w_Q \geq -1$. We make the simplifying approximation that $w_Q(t) = \text{const}$. Even though this is certainly not true for many models of dark energy, almost all models can be very well approximated by a model having a constant $w_{Q,\text{eff}}$, which is then calculated as a properly weighted mean of $w_Q(t)$ [10, 19]. With this approximation the dark energy density evolves simply as $\rho_Q \propto a^{-3(1+w_Q)}$, where a is the scale factor.

Our analysis of the present data is in many ways similar to that performed in Ref. [10]. However, in addition to the extension of the parameter space to $w_Q < -1$ we also include new data from the 2dF galaxy survey.

Finally, we discuss the prospects for measuring w_Q precisely with future high precision CMB and SN data.

II. DATA ANALYSIS

A. CMB and large scale structure

CMB data set — Several data sets of high precision are now publicly available. In addition to the COBE [20] data for small l there are data from BOOMERANG [21], MAXIMA [22], DASI [23] and several other experiments [24, 25]. Wang, Tegmark and Zaldarriaga [24] have compiled a combined data set from all these available data, including calibration errors. In the present work we use this compiled data set, which is both easy to use and

*Electronic address: steen@nordita.dk

†Electronic address: edvard@physto.se

includes all relevant present information.

LSS data set — At present, by far the largest survey available is the 2dF [26] of which about 147,000 galaxies have so far been analysed. Tegmark, Hamilton and Xu [27] have calculated a power spectrum, $P(k)$, from this data, which we use in the present work. The 2dF data extends to very small scales where there are large effects of non-linearity. Since we only calculate linear power spectra, we use (in accordance with standard procedure) only data on scales larger than $k = 0.2h \text{ Mpc}^{-1}$, where effects of non-linearity should be minimal.

The CMB fluctuations are usually described in terms of the power spectrum, which is again expressed in terms of C_l coefficients as $l(l+1)C_l$, where

$$C_l \equiv \langle |a_{lm}|^2 \rangle. \quad (1)$$

The a_{lm} coefficients are given in terms of the actual temperature fluctuations as

$$T(\theta, \phi) = \sum_{lm} a_{lm} Y_{lm}(\theta, \phi). \quad (2)$$

Given a set of experimental measurements, the likelihood function is

$$\mathcal{L}(\Theta) \propto \exp\left(-\frac{1}{2}x^\dagger [C(\Theta)^{-1}]x\right), \quad (3)$$

where $\Theta = (\Omega, \Omega_b, H_0, n, \tau, \dots)$ is a vector describing the given point in parameter space, x is a vector containing all the data points, and $C(\Theta)$ is the data covariance matrix. This applies when the errors are Gaussian. If we also assume that the errors are uncorrelated, it can be reduced to the simple expression, $\mathcal{L} \propto e^{-\chi^2/2}$, where

$$\chi^2 = \sum_{i=1}^{N_{\max}} \frac{(C_{l,\text{obs}} - C_{l,\text{theory}})_i^2}{\sigma(C_l)_i^2}, \quad (4)$$

is a χ^2 -statistic and N_{\max} is the number of power spectrum data points [28]. In the present paper we use Eq. (4) for calculating χ^2 for the CMB data. Since we also use data from the 2dF survey the total χ^2 is then given by

$$\chi^2 = \sum_{i=1}^{N_{\max,\text{CMB}}} \frac{(C_{l,\text{obs}} - C_{l,\text{theory}})_i^2}{\sigma(C_l)_i^2} + \sum_{j=1}^{N_{\max,\text{LSS}}} \frac{(P(k)_{\text{obs}} - P(k)_{\text{theory}})_j^2}{\sigma(P(k))_j^2}. \quad (5)$$

The procedure is then to calculate the likelihood function over the space of cosmological parameters. For calculating CMB and matter power spectra we have used the publicly available CMBFAST package [29]. The 2D likelihood function for (Ω_m, w_Q) is obtained by keeping (Ω_m, w_Q) fixed and marginalising over all other parameters.

As free parameters in the likelihood analysis we use Ω_m , the matter density, w_Q , the dark energy equation of state, Ω_b , the baryon density, H_0 , the Hubble parameter, n , the scalar spectral index, and τ , the optical depth to reionization. The normalisation of the CMB data, Q , and of the 2dF data, b , are taken as completely free and uncorrelated parameters in the analysis. This is very conservative and eliminates any possible systematics involved in determining the bias parameter. We constrain the analysis to flat ($\Omega_m + \Omega_Q = 1$) models, and we assume that the tensor mode contribution is negligible ($T/S = 0$). These assumptions are compatible with analyses of the present data [24], and relaxing them does not have a big effect on the final results.

TABLE I: The different priors used in the analysis.

Parameter	Prior
Ω_m	0.1-1
w_Q	-3 - -0.5
$\Omega_b h^2$	0.020 ± 0.002 (Gaussian)
h	0.72 ± 0.08 (Gaussian)
n	0.5-1.4
τ	0-1
Q	free
b	free

Table I shows the different priors used. We use the constraint $H_0 = 72 \pm 8 \text{ km s}^{-1} \text{ Mpc}^{-1}$ [$h \equiv H_0/(100 \text{ km s}^{-1} \text{ Mpc}^{-1})$] from the HST Hubble key project [30] (the constraint is added assuming a Gaussian distribution) and the constraint $\Omega_b h^2 = 0.020 \pm 0.002$ from BBN [31].

Fig. 1 then shows the 68.3% and 95.4% confidence allowed regions, corresponding to $\Delta\chi^2 = 2.31$ and 6.17 respectively.

For very negative values of w_Q the CMB and LSS constraint is independent of w_Q . The reason is that at such low w_Q the dark energy influences the CMB spectrum only via the late integrated Sachs-Wolfe effect. However, the late ISW effect decreases in magnitude as w_Q decreases. This effect can be seen in Fig. 2 where CMB power spectra are plotted for different values of w_Q .

B. Type Ia supernovae

SN data set — The SN data set used in this analysis corresponds to Fit C from the Supernova Cosmology Project as described in [32]. This is a subsample of a total of 60 SNe where two SNe are excluded as statistical outliers, two because of atypical lightcurves and two because of suspected reddening.

We use this data set to fit Ω_m and w_Q , taking advantage of the cosmology dependence of the distance-redshift

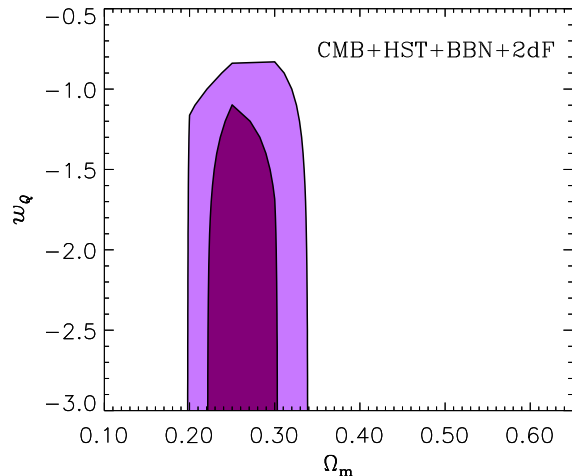


FIG. 1: The 68.3% (dark shaded) and 95.4% (light shaded) confidence allowed regions for Ω_m and w_Q using CMB, HST, BBN and LSS data.

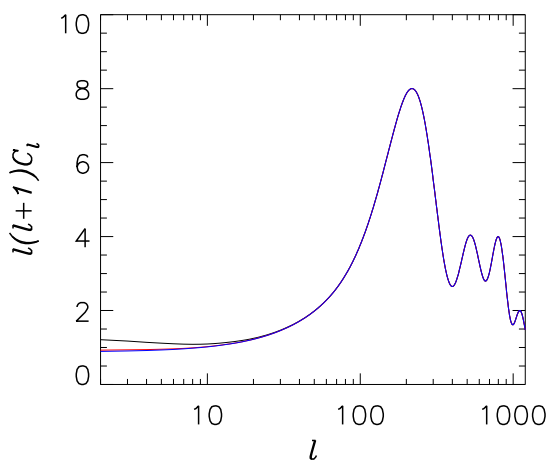


FIG. 2: Different CMB power spectra for different values of w_Q . In all cases the model parameters are those of the fiducial Λ CDM model, $\Omega_m = 0.3$, $\Omega_\Lambda = 0.7$, $\Omega_b h^2 = 0.020$, $H_0 = 70 \text{ km s}^{-1} \text{ Mpc}^{-1}$. The full line is for $w_Q = -1$, the dashed for $w_Q = -2$, and the dotted for $w_Q = -4$ (in order of decreasing C_l at low l).

relation. Type Ia SNe are very useful as distance indicators because of their high luminosities and small dispersion among their peak absolute magnitudes ($\sigma_m \simeq 0.15$). Also, they have distinct spectral lines, allowing for accurate redshift determinations.

The apparent and absolute magnitudes are related by

$$m(z) = M + 5 \log [\mathcal{D}_L(z, \Omega_m, w_Q)] - 5 \log H_0 + 25, \quad (6)$$

where $\mathcal{D}_L := H_0 d_L$ is the part of the luminosity distance

that remains after multiplying out the dependence on the Hubble constant (expressed here in units of $\text{km s}^{-1} \text{ Mpc}^{-1}$). In the low redshift limit, Eq. (6) reduces to a linear Hubble relation between m and $\log z$:

$$m(z) = \mathcal{M} + 5 \log z, \quad (7)$$

where we have expressed the intercept of the Hubble line as $\mathcal{M} := M - 5 \log H_0 + 25$. This quantity can be measured from the apparent magnitude of low redshift standard candles, without knowing the value of H_0 . Thus, with a set of apparent magnitude and redshift measurements $m(z)$ for Type Ia SNe, we can find the best-fit values of (Ω_m, w_Q) to solve the equation

$$m(z) - \mathcal{M} = 5 \log [\mathcal{D}_L(z, \Omega_m, w_Q)]. \quad (8)$$

The χ^2 is then given by

$$\chi^2 = \sum_{i=1}^n \frac{[m_i - 5 \log [\mathcal{D}_L(z_i, \Omega_m, w_Q)] - \mathcal{M}]^2}{\sigma_i^2}, \quad (9)$$

where σ_i is the statistical uncertainty for each event. We assume a flat geometry of the universe when calculating \mathcal{D}_L and marginalise over \mathcal{M} where we assume no prior knowledge.

In Fig. 3, the 68.3% and 95.4% confidence allowed regions are shown. The best-fit values are $\Omega_m = 0.45$ and $w_Q = -1.9$, indicating the possibility of a bias in the parameter determination when imposing the constraint $w_Q \geq -1$.

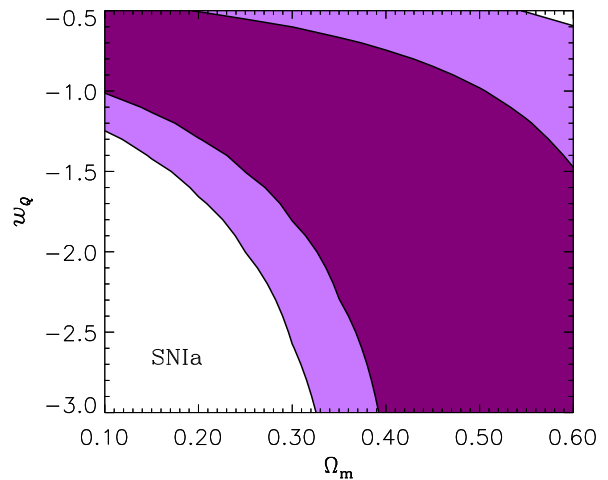


FIG. 3: The 68.3% (dark shaded) and 95.4% (light shaded) confidence allowed regions for Ω_m and w_Q using the 54 type Ia SNe from the Supernova Cosmology Project.

C. Combined constraint

When all the available data is combined, a fairly stringent bound on w_Q is obtained. The 68.3% and 95.4%

confidence combined bounds are shown in Fig. 4. For w_Q alone we find a 95.4% confidence bound of $-2.68 < w_Q < -0.78$.

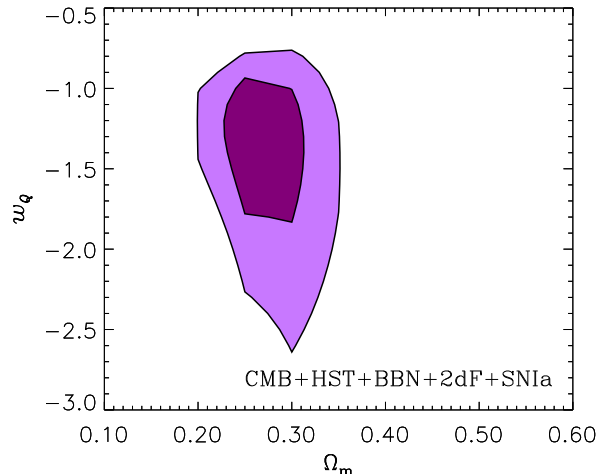


FIG. 4: The 68.3% (dark shaded) and 95.4% (light shaded) confidence allowed regions for Ω_m and w_Q using all available data.

III. DISCUSSION

A. Constraints from present data

An important point is to determine whether the relaxation of the bound $w_Q \geq -1$ significantly affects the likelihood analysis for the part of parameter space which is above $w_Q = -1$. This could be the case if the best-fit value of w_Q lies in the excluded region as is the case for the current SN data, where the best-fit value corresponds to $\Omega_m = 0.45$, $w_Q = -1.9$. For the CMB+LSS data the situation is the same, with the overall best fit being at $\Omega_m = 0.26$, $w_Q = -2.6$. In Fig. 5 we plot the the likelihood contours with the constraint $w_Q \geq -1$ imposed. In terms of w_Q alone the 95.4% confidence bound is now $-1 \leq w_Q < -0.71$.

Comparing this to the bound obtained without the constraint shows that the likelihood contours are fairly similar and that the bias is not a significant problem. Our Fig. 4 can for instance also be compared to Fig. 3 of Ref. [10]. Apart from the smaller allowed region in Ω_m because of the tighter BBN constraint and the use of the full 2dF data set, the two plots are very similar. The bound on w_Q found in Ref. [10] is $-1 \leq w < -0.73$, very similar to the constraint found in the present analysis when the constraint $w_Q \geq -1$ is imposed.

This shows both that our constrained analysis is consistent with Ref. [10] and that this previous analysis of w_Q is not seriously biased.

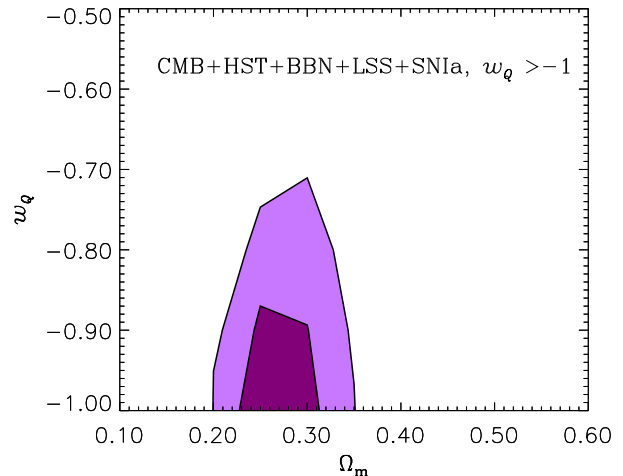


FIG. 5: The 68.3% (dark shaded) and 95.4% (light shaded) confidence allowed regions for Ω_m and w_Q using all available data and imposing the bound $w_Q \geq -1$.

The next very important point of our analysis is that one obtains a non-trivial lower bound on w_Q from the combination of CMB, LSS and SN data. From SN data alone we can infer that $w_Q \gtrsim -12$ is ruled out at the 68.3% confidence level, but combining this with CMB and LSS data tightens the bound significantly to $w_Q > -2.68$ at 95.4% confidence. It is also very interesting and perhaps somewhat suggestive that a cosmological constant lies in the 68.3% confidence allowed region.

B. Constraints from future data

The ability to constrain the equation of state parameter w_Q of a dark energy component using future CMB and Type Ia SN data have been recently investigated by a number of authors, see, e.g., [33] and references therein. Our analysis differ in the respect that we do not impose the constraint $w_Q \geq -1$ and that we use the most current anticipated data sets.

CMB data set — For CMB we use simulated data from the Planck Surveyor satellite. For simplicity we use only data from the HFI 100 GHz channel, assuming an angular resolution of 10.7 arcmin and a pixel noise of $\Delta T/T = 1.7 \times 10^{-6}$ [34]. This channel is not polarization sensitive and so our assumed data set seems conservative compared to what can be expected from the full Planck data. On the other hand we do not include foregrounds in our analysis. The simulated data is generated from an underlying flat model with the following parameters: $\Omega_m = 0.3$, $w_Q = -1$, $\Omega_b h^2 = 0.02$, $H_0 = 70 \text{ km s}^{-1} \text{ Mpc}^{-1}$, $n = 1.0$, and $\tau = 0$.

SN data set — We use simulated data sets corresponding to three year's data from the proposed satellite tele-

scope the Supernova/Acceleration Probe (SNAP; [35]) and the predicted results from the Supernova Factory Campaign (SNfactory; [36]) scheduled to start in the end of 2002.

The SNAP satellite would be capable of discovering and taking spectra of ~ 2800 Type SNe per year for redshifts $z < 1.7$. The current projected redshift distribution follows the distribution in the SNAP proposal [35] for $z < 1$ and is approximately uniform at higher redshifts [37]. The SNfactory data set consists of 200 SNe between $0.03 < z < 0.06$ and 100 SNe between $0.06 < z < 0.15$. The simulated data is generated for the same underlying model as for the CMB simulations.

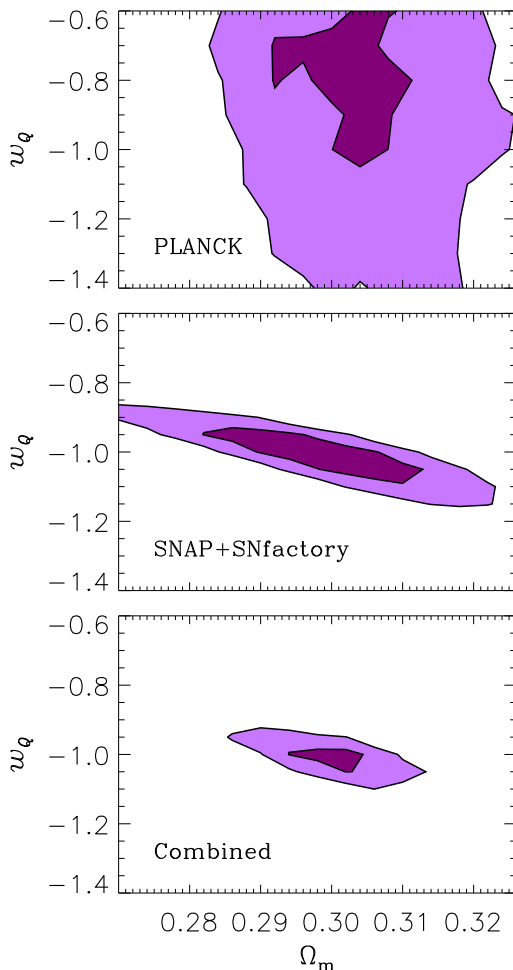


FIG. 6: The 68.3% (dark shaded) and 95.4% (light shaded) confidence allowed regions for Ω_m and w_Q using simulated data from the Planck satellite and the SNAP and SNfactory observatories.

In Fig. 6 we show a likelihood analysis based on the simulated CMB and Type Ia SN data. It is clear that again the data will complement each other, the CMB data being very sensitive to Ω_m and the SNIa data to w_Q . From the combined data set we estimate that it is possible to obtain a 95.4% confidence interval on w_Q of

roughly 0.05 relative precision in the two parameters. In this note we have neglected the possible use of multiple imaged core-collapse SNe to constrain w_Q and Ω_m , see Ref. [38].

It is important to note that the confidence regions presented only take into account statistical uncertainties. For future Type Ia SN data sets, systematic errors from, e.g., dust obscuration, luminosity evolution and gravitational lensing might be comparable to or even larger than the statistical errors. In Fig. 7 the confidence regions corresponding to the middle panel of Fig. 6 is shown if lensing effects from 90% NFW dark matter halos and 10% point masses are included in the simulated data set (generated with $\Omega_m = 0.3$ and $w_Q = -1$). It is obvious that gravitational lensing, if not taken into account, will cause an underestimation of the matter density and in order to reach the full potential of the large statistics, we need to correct for the effect, e.g., as described in [39]. For the CMB data there may also be systematic errors of a magnitude comparable to the purely statistical ones.

However, if the systematic errors can be controlled in an effective matter, we conclude that it should be possible to constrain the equation of state parameter w_Q of the dark energy to high accuracy using future CMB and SN data sets.

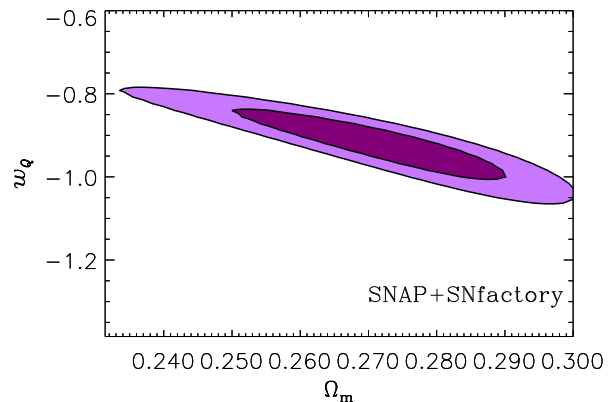


FIG. 7: The 68.3% (dark shaded) and 95.4% (light shaded) confidence allowed regions for Ω_m and w_Q using simulated data from the SNAP and SNfactory observatories, with lensing effects from 90% NFW halos and 10% point masses included. The simulated data is generated with $\Omega_m = 0.3$ and $w_Q = -1$.

Acknowledgments

We wish to thank A. Melchiorri for valuable discussions during the initial stages of the project.

-
- [1] C. Wetterich, Nucl. Phys. B **302**, 668 (1988).
- [2] P. J. Peebles and B. Ratra, Astrophys. J. **325**, L17 (1988).
- [3] C. Wetterich, Astron. Astrophys. **301**, 321 (1995) [arXiv:hep-th/9408025].
- [4] I. Zlatev, L. M. Wang and P. J. Steinhardt, Phys. Rev. Lett. **82**, 896 (1999) [arXiv:astro-ph/9807002].
- [5] L. M. Wang, R. R. Caldwell, J. P. Ostriker and P. J. Steinhardt, Astrophys. J. **530**, 17 (2000) [arXiv:astro-ph/9901388].
- [6] P. J. Steinhardt, L. M. Wang and I. Zlatev, Phys. Rev. D **59**, 123504 (1999) [arXiv:astro-ph/9812313].
- [7] Y. Wang and P. M. Garnavich, Astrophys. J. **552**, 445 (2001) [arXiv:astro-ph/0101040].
- [8] Y. Wang and G. Lovelace, Astrophys. J. **562**, L115 (2001) [arXiv:astro-ph/0109233].
- [9] C. Baccigalupi, A. Balbi, S. Matarrese, F. Perrotta and N. Vittorio, Phys. Rev. D **65**, 063520 (2002) [arXiv:astro-ph/0109097].
- [10] R. Bean and A. Melchiorri, Phys. Rev. D **65**, 041302 (2002) [arXiv:astro-ph/0110472].
- [11] P. S. Corasaniti and E. J. Copeland, Phys. Rev. D **65**, 043004 (2002) [arXiv:astro-ph/0107378].
- [12] R. R. Caldwell, arXiv:astro-ph/9908168.
- [13] T. Chiba, T. Okabe and M. Yamaguchi, Phys. Rev. D **62**, 023511 (2000) [arXiv:astro-ph/9912463].
- [14] H. Ziaeepour, arXiv:astro-ph/0002400.
- [15] V. Faraoni, arXiv:astro-ph/0110067.
- [16] A. Riazuelo and J. P. Uzan, Phys. Rev. D **62**, 083506 (2000) [arXiv:astro-ph/0004156].
- [17] A. E. Schulz and M. J. White, Phys. Rev. D **64**, 043514 (2001) [arXiv:astro-ph/0104112].
- [18] I. Maor, R. Brustein, J. McMahon and P. J. Steinhardt, Phys. Rev. D **65**, 123003 (2002) [arXiv:astro-ph/0112526].
- [19] G. Huey, L. M. Wang, R. Dave, R. R. Caldwell and P. J. Steinhardt, Phys. Rev. D **59**, 063005 (1999) [arXiv:astro-ph/9804285].
- [20] C. L. Bennett *et al.*, Astrophys. J. Lett. **464**, L1 (1996) [astro-ph/9601067].
- [21] C. B. Netterfield *et al.* [Boomerang Collaboration], arXiv:astro-ph/0104460.
- [22] A. T. Lee *et al.*, arXiv:astro-ph/0104459.
- [23] N. W. Halverson *et al.*, arXiv:astro-ph/0104489.
- [24] X. Wang, M. Tegmark and M. Zaldarriaga, arXiv:astro-ph/0105091 (WTZ).
- [25] X. Yu *et al.*, arXiv:astro-ph/0010552.
- [26] J. Peacock *et al.*, Nature **410**, 169 (2001).
- [27] M. Tegmark, A. J. S. Hamilton and Y. Xu, arXiv:astro-ph/0111575.
- [28] S. P. Oh, D. N. Spergel and G. Hinshaw, Astrophys. J. **510**, 551 (1999).
- [29] U. Seljak and M. Zaldarriaga, Astrophys. J. **469**, 437 (1996).
- [30] W. L. Freedman *et al.*, arXiv:astro-ph/0012376.
- [31] S. Burles, K. M. Nollett and M. S. Turner, arXiv:astro-ph/0010171.
- [32] S. Perlmutter *et al.*, Astrophys. J. **517**, 565 (1999).
- [33] M. Goliath, R. Amanullah, P. Astier, A. Goobar and R. Pain, Astron. Astrophys. **380**, 6 (2001)
- [34] See the Planck homepage <http://astro.estec.esa.nl/SA-general/Projects/Planck/>
- [35] SNAP Science Proposal, available at <http://snap.lbl.gov>.
- [36] G. Aldering, *et al.*, Supernova Factory Webpage, <http://snfactory.lbl.gov>.
- [37] E. Linder, private communication.
- [38] A. Goobar, E. Mörtsell, R. Amanullah and P. Nugent, accepted for publication in Astron. Astrophys.
- [39] R. Amanullah, E. Mörtsell and A. Goobar, arXiv:astro-ph/0204280.